

Consolidation of sediments discharged from the Yellow River: implications for sediment erodibility

Xiaolei Liu · Yonggang Jia · Jiewen Zheng ·
Xiujuan Yang · Hongxian Shan

Received: 13 December 2011 / Accepted: 21 January 2013 / Published online: 7 February 2013
© Springer-Verlag Berlin Heidelberg 2013

Abstract Consolidation processes acting on an intertidal mudflat in the Yellow River delta, China, were investigated using field and laboratory experiments. The dissipation of excess pore pressure was examined in an excavated experimental plot to characterise the short-term consolidation of sediments discharged from the Yellow River. Changes in sediment strength were monitored over a 5-year period, together with measurements of physical and mechanical properties using laboratory experiments. In addition, the erodibility of silty sediments under wave loading conditions was also tested in the field. Results showed that sediments discharged from the Yellow River experienced a high rate of consolidation after initial deposition. Excess pore pressure dissipated completely after approximately 45 to 51 h. Sediments were then in a state of quasi-overconsolidation and showed heterogeneity in strength. Hydrodynamic action appears to be crucial to sediment consolidation in the primary period and plays a decisive role in the development of a stiff stratum. Changes in sediment strength due to wave-induced secondary modifications over varying temporal and spatial scales are consistent with variations in sediment erodibility. This factor should be considered in the development of erosion models for intertidal mudflat sediments.

Responsible Editor: Han Winterwerp

This article is part of the Topical Collection on the *11th International Conference on Cohesive Sediment Transport*

X. Liu · Y. Jia · J. Zheng · H. Shan
Key Laboratory of Marine Environmental & Ecology, Ministry of Education, 266100, Qingdao, China

Y. Jia (✉) · H. Shan
Faculty of Environmental Science & Engineering, Ocean University of China, 266100, Qingdao, China
e-mail: yonggang@ouc.edu.cn

X. Yang
Architecture Engineering Department, Wenjing College Yantai University, 264005, Yantai, China

Keywords Consolidation · Erodibility · Sediment strength · Hydrodynamics · Intertidal flats · Yellow River delta

1 Introduction

Intertidal flats are an important component of the coastal zone, providing important ecosystem functions, such as nursery habitats for fish and crustaceans and nesting and feeding areas for migratory birds. They support biodiversity, filter contaminants, dissipate water energy, and offer intrinsic values, such as aesthetics and education (Eisma 1998). The preservation and management of these environments have become significant due to their ecological and geomorphological importance to the local community, researchers, and dependent industries (e.g. fisheries and tourism; Costanza et al. 1997).

The nature of fine-grained, cohesive sediments (muds) plays a significant role in the morphological dynamics of tidal flat systems (Anthony 2004; Capo et al. 2006). Different studies have aimed to identify and understand mechanisms of deposition and erosion and to predict the morphological behaviour of intertidal mudflats (Amos et al. 1992; Allen 1997; Gouleau et al. 2000; Janssen-Stelder 2000; Wang 2003; Deloffre et al. 2005; Quaresma et al. 2007). However, physical properties and the state of deposited sediments can be affected by biological and hydrodynamic processes (Richardson et al. 2002). Erodibility changes in intertidal mudflat sediments during consolidation were reported by Meng et al. (2010), who observed that the critical erosion shear stress for freshly deposited sediments correlated positively with bulk density and negatively with water content. Thus, consolidation of intertidal mudflat sediments provides erosion resistance for the morphodynamic behaviour of intertidal mudflats.

The Yellow River is known for its extremely heavy sediment load (Milliman and Meade 1983) of approximately 1.0–1.1

billion tons/year, which is second only to the Amazon River (Milliman and Syvitski 1992). Approximately 80 % of these sediment loads is deposited rapidly in the estuary delta (Bornhold et al. 1986; Saito et al. 2001). Sediment sedimentation to the seabed can reach 100 mm per hour during floods with extremely high sediment concentrations (Ren and Shi 1986). However, water and sediment discharges have been decreasing steadily over the past 30 years due to climate change and human activities, which has led to coastal erosion in most of the delta region, with the exception of a small area around the river mouth (Wang et al. 2007a). The dynamic behaviour of mudflat sediments is driven by complex interactions between oceans and land over varying spatial and temporal scales (Talke and Stacey 2003). Sediment consolidation of intertidal mudflats in the Yellow River delta is controlled by these interactions and feedbacks of biological, physical, sedimentary, and chemical properties of the bed, as well as by prevailing atmospheric and hydrodynamic forces.

Previous field investigations (Keller et al. 1990; Lu et al. 1991; Jia et al. 2011) have identified the inhomogeneous mechanical properties of superficial sediments in the subaqueous Yellow River delta. Morgan et al. (1963) and Coleman et al. (1978) initially explained this phenomenon in the subaqueous Mississippi River delta as a native mode characterised by an orderly repetition of depositional events. However, secondary variations in sediment properties affected by marine hydrodynamics also could explain the non-homogeneity (Davidson-Arnott and Langham 2000; Wheatcroft and Borgeld 2000). In recent years, more studies have found that the dynamic response of seabed sediment to wave loading is complicated in the Yellow River delta (Zheng et al. 2011; Liu et al. 2013); unfortunately, less work has focused on the unique influence of wave loading to sediment consolidation, although it has been discussed by certain researchers (Jia et al. 2011). Seabed sediments in this region are prone to liquefaction, and seabed properties and topography can vary greatly under wave loading (e.g. van Maren et al. 2009; Jia et al. 2012). Therefore, we cannot adopt traditionally constructed models for consolidated sediments to study the wave-induced behavioural characteristics of sediment erodibility.

Considering the particularities and complexities in characterising the dynamic behaviour of intertidal flats, this paper focuses on consolidation processes observed on intertidal mudflats in the Yellow River delta and discusses its implications for sediment erodibility. The objectives are to:

1. Quantify the variability in physical and mechanical properties of sediments discharged from the Yellow River over varying temporal and spatial scales.
2. Determine the impacts of hydrodynamics on marine deposited sediments.
3. Determine how hydrodynamic actions affect sediment erodibility by changing sediment properties.

2 Field site

The field observation site was located within an intertidal mudflat on the western shore of the Bohai Sea (N 38°08' 11.3", E 118°46'58.8"), which is located on the Diaokou River and Shenxiangou sub-delta of the Yellow River delta (Fig. 1). This sub-delta was formed from 1953 to 1976 when the Yellow River flowed along the Diaokou River and Shenxiangou channels and lies north of the present mouth of the Yellow River (Fan et al. 2006). The deltaic underwater slope in this area, consisting of a tidal flat and its lower portion, is so gentle (generally <0.6°) that the exposed tidal flat can extend several kilometres during low tide, providing convenient conditions for field sampling.

The intertidal mudflat experiences an irregular semidiurnal tide, with a tidal range from 0.84 to 1.08 m (Shi and Zhao. 1985). The tidal current runs north–south, which is approximately perpendicular to the river runoff flow. The tidal current can reach 1.0 to 2.0 m/s (Wang and Liang 2000). Waves in this area are mostly driven by winds in the Bohai Sea, and wave characteristics thus have distinct seasonality associated with the monsoon (Wang et al. 2007b). Average wave heights are approximately 20 cm in normal sea conditions. Strong erosion and scour occur in this coastal area, and the coastline retreats landward, which is mostly caused by winter storm waves and partially by tidal currents (Yang et al. 2011a).

Mudflat sediments are characterised as silty loam. The soil contains 0.4 % to 5.2 % of sand, 84.5 % to 92.3 % of silt, and 6.2 % to 15.1 % of clay, with water content ranging from 23.8 % to 29.1 %, bulk density from 1.91 to 1.94 g/cm³, and void ratio from 0.73 to 0.81. The major detrital minerals of sediments are quartz, feldspar, calcite, and dolomite, which account for 75.8 % of the total mineral composition. The clay minerals are illite, chlorite, kaolinite, and montmorillonite, which make up the rest (24.2 %) of the total mineral composition (Table 1).

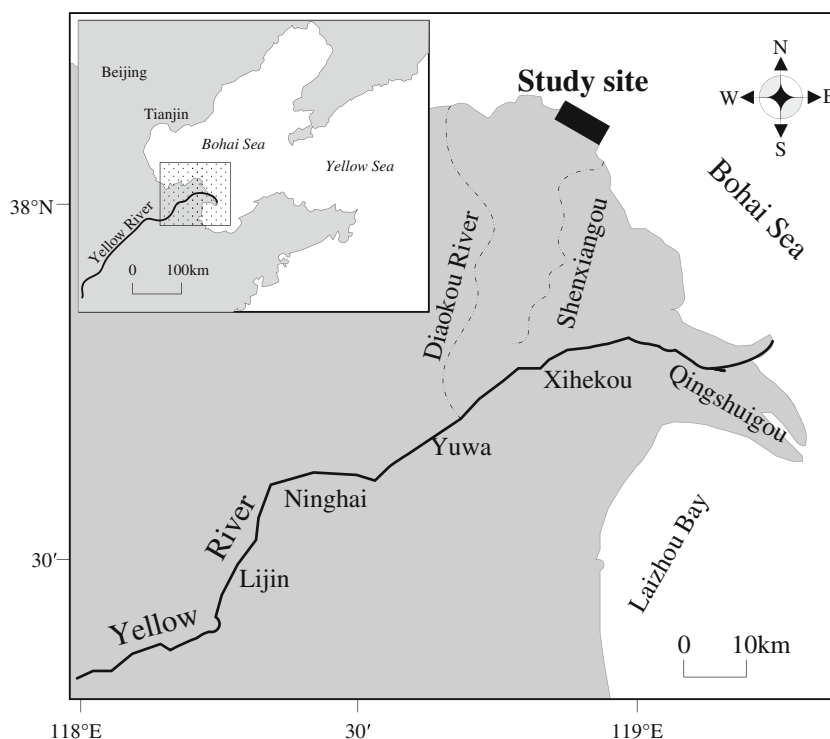
3 Materials and methods

3.1 Consolidation experiments

3.1.1 Experiment 1

To study the dynamic response of rapidly depositing sediments to wave and tidal effects, a test pit (2×1×1 m; Figs. 2 and 3a) was excavated on the intertidal mudflat on April 6, 2004. The excavated soil was air-dried and ground before being used in the field experiment. Some of the air-dried soil was weighed and placed in a container. Local sea water was then added into the container and mixed with the soil until it became a homogeneous slurry (Fig. 3b), with an estimated

Fig. 1 The Yellow River estuary and study site



sediment concentration of 200 kg/m^3 . Suspended sediment concentrations (SSC) during extreme flood events may reach 222 kg/m^3 at the Yellow River mouth (Keller and Prior 1986), so the slurry was backfilled into the test pit to simulate rapid deposition and consolidation processes (Fig. 3c). Pore water pressure, sediment strength, and other physical and mechanical properties of deposited sediments were measured over varying spatial and temporal scales.

Devices for measuring pore water pressure in the field were designed and manufactured by the Nanjing Hydraulic Research Institute. Four piezoresistive pressure sensors ($20 \times 60 \text{ mm}$) were connected to these devices and installed at depths of 0, 30, 50, and 75 cm.

To characterise consolidation and long-term variations in soil strength, in situ measurements, including the light penetration test (LPT) and vane shear test (VST), were performed in and out of the test pit in April 2004, August 2005, September 2006, and July 2008. The four sampling events were conducted on the completely exposed mudflat during neap tides. LPT was conducted using a portable cone penetration probe, with a diameter of approximately 15 mm (WG-V, Shenyang Jianke Instrument Research Institute,

China), as described in Jia et al. (2011). VST was conducted using a CLD-3 Electrical Vane Tester, and data were acquired using the DN-1 system (Nanguang Geological Instrument Company, China).

Soil samples were collected manually from both the test pit and neighboring undisturbed seabed using coring tubes (7.5 cm diameter and 1.0 m length). The sediment cores were capped at both ends and maintained in a wet chamber to avoid losing water content before careful transport to the geotechnical laboratory. Several cores were collected from the same site to obtain sufficient material for the various analyses, such as water content, bulk density, specific gravity, compressibility modulus, preconsolidation pressure, etc. All soil samples were tested in triplicate to obtain mean results and allow discussion of temporal variations in sediment physical and mechanical properties.

3.1.2 Experiment 2

To quantify the contributions of marine dynamics on sediment consolidation, an identical test pit was excavated and refilled with homogeneous slurry on July 13, 2008. An iron

Table 1 Major detrital mineral and clay mineral composition of the mudflat sediment within depth of 1 m

Detrital mineral composition (%)					Clay mineral composition (%)				
Quartz	Feldspar	Calcite	Dolomite	Total	Illite	Chlorite	Kaolinite	Montmorillonite	Total
43.68	20.71	9.47	1.94	75.8	13.67	4.44	5.78	0.31	24.2

The sediment mineralogy was analysed using the X-ray diffraction (XRD) technique

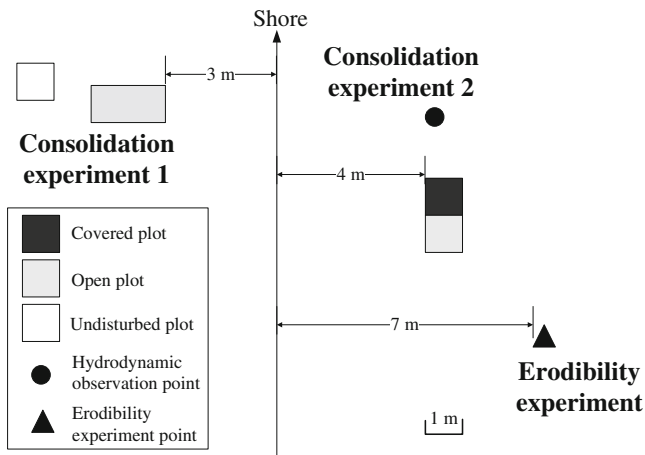


Fig. 2 Plan view of layout of experimental plots at the field site

sheet (1.0 m length, 1.0 m width, and 0.10 m height) was placed over the west surface of the test pit and secured by large stones at the corners. The test pit was thus divided into open and covered plots with dimensions of $1 \times 1 \text{ m}^2$ (Figs. 2 and 3d). The covered plot was protected from both currents and high frequency pressure fluctuations due to waves (Davidson-Arnott and Langham 2000). Hydrodynamic and sediment strength measurements were conducted for both plots during the experiment (July 13 to July 30, 2008).

Hydrodynamic measurements were collected using a wave and tide recorder (TWR-2050; RBR Company, Canada) and a kinemometer (ALEC Company, Japan),

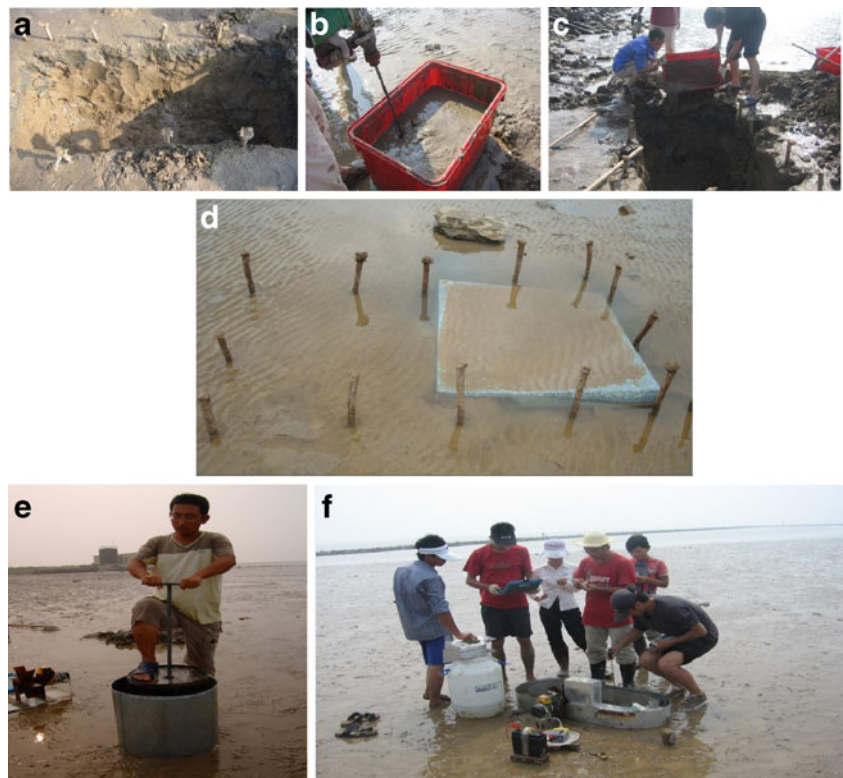
which were both fixed to a bearing rack placed on the mudflat to measure tidal waves and current velocities for 18 days. LPT and VST were performed on the open and covered plots to obtain penetration resistance, undrained shear strength and sediment sensitivity in the test pit.

Cylindrical cores were also collected and treated in the same way as in Experiment 1, and then carefully transported to the laboratory by car. A stereoscopic microscope (SMZ 1500, Nikon, Japan) was used to characterise the soil microstructure. Central sections of the core samples were selected for the microstructure test to minimise the effects of sampling and transportation disturbance. Continuous observations were conducted on the air-dried sediment samples sorted by depth, and typical components were photographed under high magnification.

3.2 Erodibility experiments

To quantify the effects of waves on sediment erodibility, wave simulations and recirculating flume experiments were conducted in July 2008 with mudflat surfaces where bioturbation was minimal (Fig. 2). Wave loadings of different periods were first simulated using a wave-producing device (Fig. 3e) to prepare different sediment beds for the erodibility experiments. For each simulated wave loading condition, the erodibility experiment was performed using a recirculation flume (Fig. 3f), which allowed the threshold velocity and critical shear stress to be determined. The undrained

Fig. 3 Photos of: **a** test pit ($2 \text{ m} \times 1 \text{ m} \times 1 \text{ m}$) excavated on the intertidal mudflat, **b** slurry stirring in the container, **c** slurry backfilling in the test pit, **d** covered plot and open plot in consolidation experiment 2 at the field site, **e** wave loading simulations in erodibility experiment, and **f** recirculating erosion flume experiment



shear strength and penetration resistance were also evaluated for the surface sediment.

As described by Zheng et al. (2011), wave loading was simulated using a wave-producing device (Fig. 3e) by artificially driving the handle downward at a constant speed. Action cycle and cycle number were controlled manually using a stopwatch. The cycle numbers applied to sediments during this study were 0, 10, 20, 30, 40, 50, and 60, each for the same period of 8 s. The magnitude of the simulated wave loading exerted on the superficial sediment was ~4 kPa. Variability in the characteristics of test parameters for different cycle numbers was not significantly different (Table 2) before physical experiments were conducted. For each simulated loading condition, sediment strength measurements were performed after the wave loading simulating test, along with erodibility experiments.

Sediment erodibility was determined in a 1.2-m-long, aluminum, recirculating flume filled with seawater (Fig. 3f) and designed and constructed based on a mobile recirculating flume (Black and Cramp 1995). The main channel had a width of 0.1 m and a height of 0.15 m. The test section was 0.25 × 0.10 m, into which 2 cm of sediment was inserted and included surface sediments exposed to wave loading. The flow rate ranged from 0 to 50 cm/s and was induced by rotation of a propeller located at the opposite side of the flume and connected to an adjustable electric motor. Flow measurements were conducted with an LGY-II current meter, which auto-recorded the average velocity and was placed at the front of the test section. The measurement accuracy of the current meter is 0.01 cm/s. The current speed in the aluminum channel was changed at least three times, and erosion at each speed continued for approximately 5 min until turbidity in the channel was constant or decreasing.

Methods for determining the threshold velocity from the erodibility experiments were discussed previously (Zheng et al. 2011). The linear correlation between current velocity

and erosion flux was calculated according to turbidity (Neumeier et al. 2006). The background erosion flux was then used to obtain the threshold velocity for the seabed. The critical shear stress for each simulated wave loading condition was calculated as follows:

$$\frac{u}{u_*} = 5.5 + 5.75 \lg\left(\frac{yu_*}{\nu}\right) \tag{1}$$

$$\tau_0 = \rho u_*^2 \tag{2}$$

Where τ_0 is the critical shear stress of the bed, P is the seawater density (1.025 g/cm³ here), u_* is the friction velocity, u is the threshold velocity, y is the location of the flow meter probe (0.015 m here), and ν is the kinetic viscosity coefficient of seawater ($\nu=1.01 \text{ m}^2/\text{s}$; Zheng et al. 2011).

4 Results

4.1 Consolidation experiment 1

4.1.1 Excess pore water pressure variation with time after sediment deposition

Pore water pressure was measured to investigate the consolidation of rapidly deposited sediments between April 11 and April 15, 2004 (Fig. 4). These data showed that excess pore pressure at each depth was highest immediately after the backfill, which agreed with the total stress due to self-weighting of the covered sediments. The excess pore pressure was 2.82 kPa at 30 cm, 4.71 kPa at 50 cm, and 6.52 kPa at 75 cm, which reflects a generally linear increase with depth (Fig. 4). The excess pore pressure dissipated rapidly in the first 2 h, and dissipation was fastest at 75 cm; the degree of consolidation was 0.74. The excess pore pressures showed vertical heterogeneity with depth within the seabed

Table 2 Natural properties of the surficial sediment for different cycle numbers before wave loading action

No. of cycles	Physical parameters				Sediment components				Mechanical parameters	
	Wet bulk density ($\times 10^3 \text{ kg} \cdot \text{m}^{-3}$)	Dry bulk density ($\times 10^3 \text{ kg} \cdot \text{m}^{-3}$)	Water content (%)	Void ratio	Average grain diameter (mm)	Clay content (%)	Silt content (%)	Sand content (%)	Undrained shear strength (kPa)	Penetration resistance (N)
0	19.5	15.4	26.67	0.75	0.026	19.5	75.2	5.3	14.20	4.89
10	19.9	15.7	26.5	0.72	0.03	19.5	75.0	5.5	14.62	5.02
20	19.6	15.6	26.53	0.75	0.036	19.4	75.3	5.3	13.90	4.90
30	19.2	15.3	26.5	0.78	0.037	19.4	75.1	5.5	14.00	4.90
40	19.5	15.4	26.81	0.67	0.032	19.5	75.2	5.3	14.00	4.49
50	19.4	15.3	26.44	0.63	0.033	19.7	75.3	5.2	13.82	4.95
60	19.2	15.2	26.42	0.68	0.032	19.6	75.4	5.2	14.72	4.70

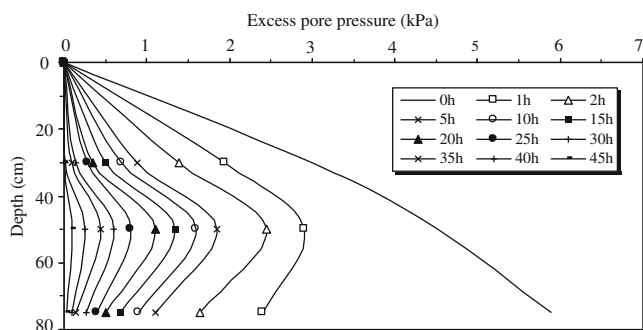


Fig. 4 Depth distribution curves of excess pore pressure at different times. Values are the differences between field measurement readings and the static water pressure at the depth where the sensor was installed

during consolidation. Sediment deposited by the Yellow River all at once was consolidated normally until the excess pore pressure dissipated completely after approximately 45 to 51 h. This consolidation process may last longer if new sediment layers are deposited over partially consolidated sediment due to additional excess pore pressure; i.e. no significant accumulation of excess pore pressure was observed due to the small waves during the experiments.

4.1.2 Strength variation with time after sediment deposition

Temporal and spatial variations in sediment strength were observed for interpretation of consolidation processes in rapidly deposited sediments (Figs. 5 and 6). The results from the short-term VST in April 2004, showed that the consolidation pressure increased with depth, and, as a consequence, the undrained shear strength increased roughly linearly with depth. Along with dissipation of the excess pore pressure, the undrained shear strength increased continuously. The excess pore pressure dissipated completely in the last 2 days (i.e. April 14 and 15), which coincided with a significant increase in the undrained shear strength at 30 cm below the seabed surface (Fig. 5). At this depth, the undrained shear strength of undisturbed soils was two to three times higher than in soils in

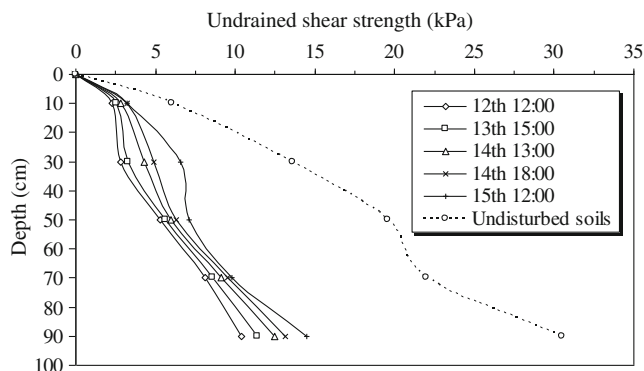


Fig. 5 Depth profile of the temporal variation of sediment undrained shear strength from VST in April 2004

the test pit on April 15, although consolidation of deposited sediments in the test pit had been completed.

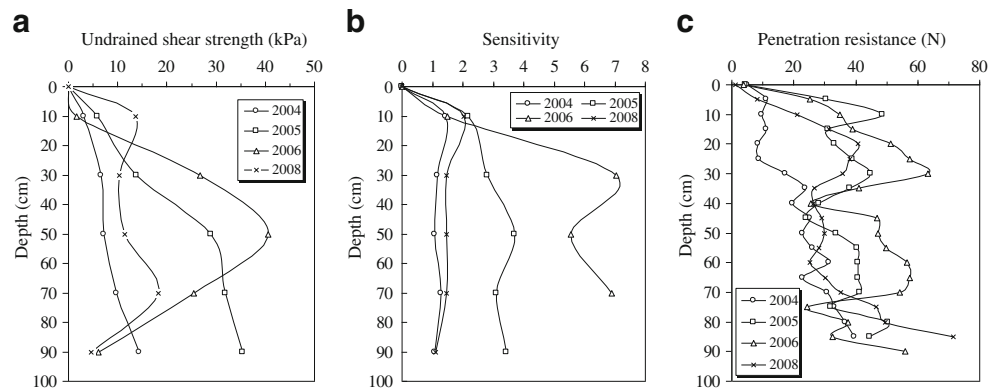
Figure 6 shows the depth profiles from long-term VST and LPT (i.e. undrained shear strength, sensitivity and penetration resistance) conducted in April 2004, August 2005, September 2006, and July 2008. These results showed that sediment undrained shear strength in the test pit varied near-linearly with depth in 2004. However, undrained shear strength increased distinctly in 2005 versus 2004, especially for soils below 50 cm. The undrained shear strength in 2006 was highest (40.5 kPa) at 50 cm, where a stiff stratum had formed. However, the undrained shear strength was significantly lower in 2008, and soils in the test pit became relatively uniform, with strengths from approximately 10 to 20 kPa (Fig. 6a). From 2004 to 2005, the mean sensitivity of soils in the test pit increased from 1.2 to 2.8, which are in the low to medium range, respectively. In 2008, sensitivity decreased to within the low value range (Fig. 6b). Similar phenomena were also observed for LPT results over time, where the measured penetration resistance increased from 2004 to 2006 and decreased significantly thereafter (Fig. 6c). It is clear that large variations in the strength of deposited sediments can occur on a timescale of years.

4.1.3 Changes in physical and mechanical properties after sediment deposition

Differences in the physical and mechanical properties between undisturbed soils and test pit soils from April 2004 are shown in Fig. 7. The undisturbed soils were more dense and had lower compressibility than test pit soils. The pre-consolidation pressure and overconsolidation ratio (OCR) of the undisturbed soils were 1 to 2 times higher than those of test pit soils. Differences in the undrained shear strength (Fig. 7) also revealed that undisturbed soils had a stronger structure than test pit soils.

Basic soil engineering tests were performed on soil samples up to 1 m depth to investigate long-term changes in physical and mechanical properties after sediment deposition. Bulk density, water content, void ratio, compressibility modulus and preconsolidation pressure of soils in the test pit were measured in April 2004, August 2005, September 2006, and July 2008 (Fig. 8). Soils at different depths in the test pit varied significantly over time. Water content was lower in the beginning, increased for a time and then decreased again at the end. Conversely, bulk density started at a high level, decreased for a time and then increased at the end. These patterns suggest that sediments deposited in the test pit experienced drained consolidation–fluidisation–drained consolidation from 2004 to 2008. At the same time, the preconsolidation pressure of test pit soils increased significantly, which suggests transformation from underconsolidation to overconsolidation over a long time scale.

Fig. 6 Depth profiles of results from long-term VST and LPT conducted in April 2004, August 2005, September 2006, and July 2008, respectively: **a** undrained shear strength, **b** sensitivity, and **c** penetration resistance



4.2 Consolidation experiment 2

4.2.1 Intertidal mudflat hydrodynamics

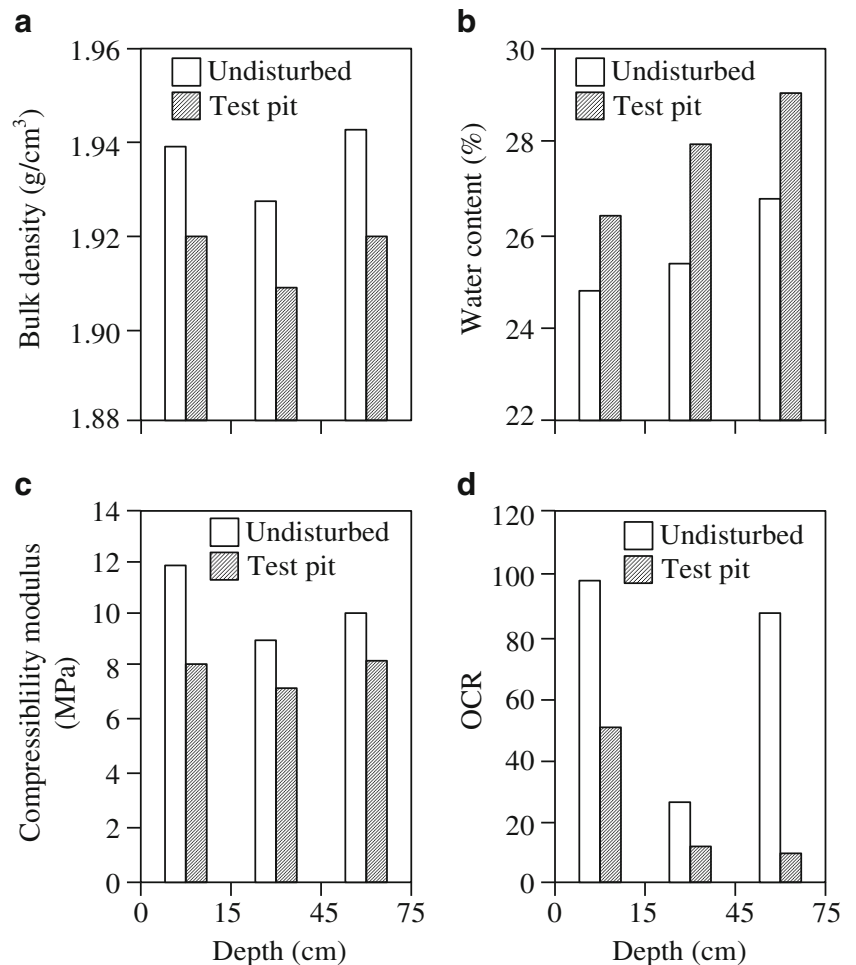
Hydrological data obtained from continuous observations of waves and currents between July 13 and July 30, 2008, are shown in Table 3. During this time, current velocity was low, with maximum and average velocities of 34.8 and 18.7 cm/s, respectively. These measurements were collected from a water depth of 0.6 to 1.0 m, with water temperature > 24 °C. $H_{1/3}$

ranged from 2 to 24 cm, with an average of 4 cm, and the wave period ranged from 4 to 6 s.

4.2.2 Strength changes in covered plot

Temporal and spatial changes in sediment strength of both the covered and open plots were measured between July 13 and July 30, 2008 (Fig. 9). The results from the covered plot show that undrained shear strength increased with time and had a linear relationship with depth, which demonstrates the

Fig. 7 Histogram showing the physical and mechanical properties of intertidal mudflat sediments (the undisturbed soils and soils in the test pit) measured in April 2004: **a** bulk density, **b** water content, **c** compressibility modulus, and **d** overconsolidation ratio (OCR)



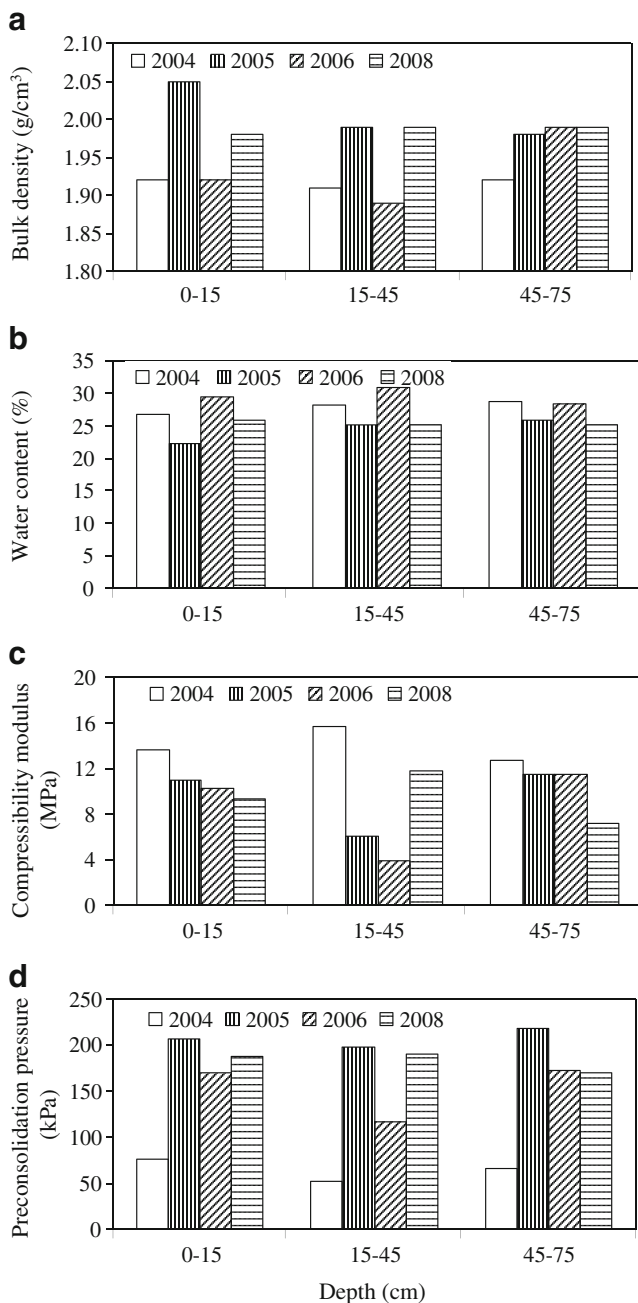


Fig. 8 Histogram showing the physical and mechanical properties of soils in the test pit measured, respectively, in April 2004, August 2005, September 2006, and July 2008: **a** bulk density, **b** water content, **c** compressibility modulus, and **d** preconsolidation pressure

characteristic of gravity consolidation (Fig. 9a). Sensitivity increased gradually with time and changed slightly with depth (mean=2.0), which can be classified as medium-low sensitivity sediment (Fig. 9b). The pattern of changes in penetration resistance was similar to that of undrained shear strength; i.e. a slight increase with time and an approximate linear relationship with depth influenced by the self-weighting consolidation pressure (Fig. 9c).

Table 3 Intertidal mudflat hydrodynamic data (including current velocity, water temperature, significant wave height, and wave period) for the measuring period: from July 13 to July 30, 2008

	Water temperature ($^{\circ}\text{C}$)	Water depth (m)	$H_{1/3}$ (cm)	Current velocity (cm/s)
Maximum	30	1.0	24	34.8
Minimum	24	0.6	2	0.5
Mean	27	0.8	4	18.7

4.2.3 Strength changes in the open plot

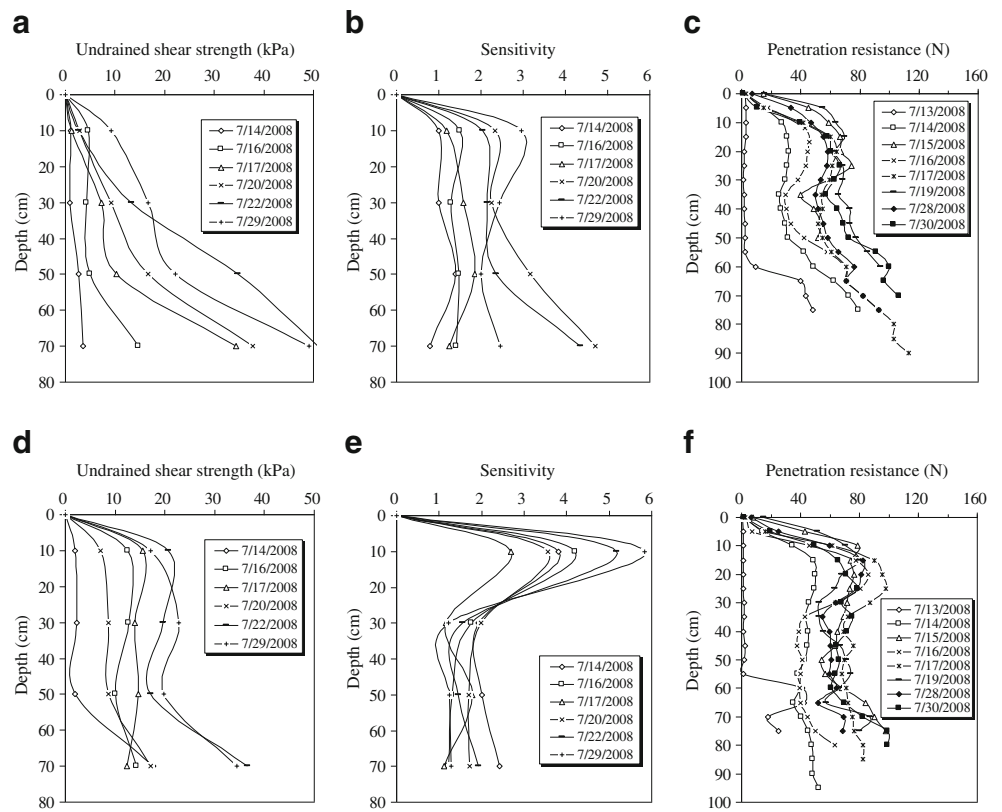
Results from the open plot allow evaluation of the behaviour of sediment strength under different hydrodynamic conditions (Table 3) and reflect consolidation of sediments affected by currents and wave-induced, high frequency pressure fluctuations. Penetration resistivity increased rapidly in the first 2 days and reached 78.9 N in the surface layer (i.e. to 10 cm depth). The overall increase in penetration resistance was low, and the 10 to 30 cm layer had the largest increase and a peak value of 97.7 N (Fig. 9f). Likewise, the undrained shear strength of sediments in the open plot increased with time, and the inhomogeneous phenomenon was observed vertically; the highest value was observed at 30 cm for the first few days of the experiment (Fig. 9d). In addition, inhomogeneous variations occurred with depth for sediment sensitivity. Above 30 cm, sensitivity increased significantly (mean=4.2), and these sediments can be classified as high-sensitivity sediment. Sediments below 30 cm had stable sensitivity (mean=1.6), which can be classified as low-sensitivity sediment (Fig. 9e). Thus, sediment strength in the surface layer (above 30 cm) was notably influenced by hydrodynamic conditions.

4.3 Erodibility experiments

In the field erodibility experiments, no linear relationships were observed for variations in sediment erodibility and correlated geotechnical parameters at the cycle number of the wave loading; the tested parameters for surficial sediments in the field varied differently under different wave loading actions (Fig. 10).

The results illustrated that sediment erodibility (i.e. threshold velocity and critical shear stress) and strength (i.e. undrained shear strength and penetration resistance) both decreased with the cycle number of wave loading in the initial stages of the wave simulation experiment. A sharp decline occurred in sediment erodibility and strength at cycle number 20, suggesting that fluidisation occurred in surface sediments. However, sediment erodibility and strength at cycle number 40 are higher than those of preceding cycle numbers. This pattern can likely be explained by

Fig. 9 Plots of temporal and spatial changes in the strength of sediments in the covered plot and the open plot over the experiment period between July 13 and July 30, 2008: **a** undrained shear strength for the covered plot, **b** sensitivity for the covered plot, **c** penetration resistance for the covered plot, **d** undrained shear strength for the open plot, **e** sensitivity for the open plot, and **f** penetration resistance for the open plot



consolidation accompanied by dissipation of excess pore pressure. Higher cycle numbers had comparatively little influence, except for the unique plot at cycle number 40 (Fig. 10). Thus, sediment erodibility and strength did not decrease with increasing cycle numbers of wave loading in field experiments. When the cycle number reaches a threshold, sediment erodibility, and strength will be stable, with nearly unchanged mechanical properties, which may result from wave-induced liquefaction (Lambrechts et al. 2010). Variations in sediment strength with the cycle number of

wave loading were consistent with sediment erodibility. It should be noted that amplitude of the wave loading produced by the self-designed wave producer is only ~4 kPa. In reality, for the waves in 5-year return period in the Yellow River estuary, wave pressure can reach ~17 kPa at the water depth of 8 m, and ~20 kPa for the waves in 50-year return period (Chang 2009). Therefore, it can be inferred that wave-induced sediment liquefaction can be considered as the main mechanism for the variation of sediment erodibility under waves.

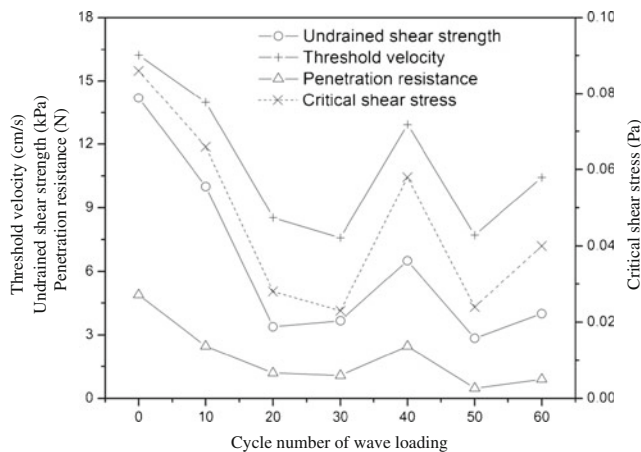


Fig. 10 Variations in the threshold velocity and critical shear stress for erosion, undrained shear strength, and penetration strength with the cycle number of wave loading in field experiments

5 Discussion

5.1 Sediment consolidation behaviour

The consolidation of cohesive sediment requires the generation of physical stresses sufficient to expulse water from interstitial spaces and the deformation of the clay mineral fabric (Berlamont et al. 1993). Many studies have shown that some offshore deposits are consolidating, losing water content, decreasing the void ratio and gaining shear strength, due to the effects of the overburden pressure (Busch and Keller 1982; Davidson-Arnott and Langham 2000; Dias and Alves 2009; Endler 2009). Natural sediment consolidation in the Yellow River delta can last several decades after sub-delta abandonment (Shi et al. 2007). However, excess pore pressure dissipation curves from the

field consolidation experiments clearly show that consolidation of rapidly deposited sediments from the Yellow River is completed in a period of 45 to 51 h (Fig. 4). Short-term variations in sediment strength suggest that undrained shear strength will increase during the dissipation of excess pore pressure, with no significant wave events during the experiment in 2004 (see Fig. 5). Sediment strength also increased slowly during normal consolidation in the covered plot. However, sediment strength in the test pit continued to increase after complete dissipation of excess pore pressure, and the soils in the test pit were thixotropic (Fig. 5). This pattern is due to the formation of soil structure, which is mainly influenced by cementation and the sedimentary environment (Gong et al. 2000).

Deposited sediments consolidate rapidly, so this discussion is further focused on how and why sediment geotechnical parameters change over long time scales. The results from VST and LPT (Fig. 6) suggest that sediment strengths in the test pit generally increased from 2004 to 2006 and decreased significantly thereafter; heterogeneity also increased with depth. Sediment physical and mechanical measurements (Fig. 8) provide indirect evidence that sediments deposited in the test pit experienced sequential drained consolidation–fluidisation–drained consolidation from 2004 to 2008. Compared to the results from 2004, deposited sediments were transformed from under-consolidation to over-consolidation over a long time scale. South- and southeastward sediment dispersal paths prevail near the river mouth (Qiao et al., 2010), suggesting that the recent Yellow River discharge record has little effect on long-term sediment deposition in this region. The long-term contribution of depositional events to temporal variations in sediment properties was not quantified in the present study. However, relatively weak depositional events occur in the study area, and the sediment deposition flux is only 0.1 mm/a for the northern, abandoned lobe of the Yellow River (Yang et al. 2011b). Therefore, possible explanations for temporal variations in sediment properties and consolidation state may be related to: (a) the presence of bacteria and benthic fauna, which can change the geological properties of sediments in the estuarine intertidal zone and promote heterogeneity (Shan et al. 2009); and (b) long-term, marine hydrodynamic actions on the intertidal mudflat. The latter is the primary topic of this article and will be discussed in the following sections.

5.2 Contribution of hydrodynamic action

The intertidal sediment suffers from long-term and repeated hydrodynamic actions due to waves and tides. The wave-induced stresses resulting from high-frequency waves have the most important impacts on seabed dynamics. The contribution of hydrodynamics to sediment strength during

consolidation (Fig. 11) can be characterised by the undrained shear strength increments of seabed sediments due to the cyclic wave-induced stresses measured in the covered and open plots between July 13 and July 30, 2008. Hydrodynamic factors appear to be crucial to sediment consolidation initially, which demonstrates the effect of hydrodynamics on enhancing sediment strength. The hydrodynamic influence is reduced at >30 cm depth and the sediment layer most affected by hydrodynamics is the 10 to 30 cm layer, where the stiff stratum is located (Fig. 9). The contribution of hydrodynamics to sediment strength is nearly seven times larger than the impact of self-weighting of sediments discharged from the Yellow River. This hydrodynamic impact is also evident in the microstructure photos (Fig. 12). In the region of little hydrodynamic influence, sediment particles are characterised by loose structures, and no obvious differences in particle composition at different depths were observed (Figs. 12a, c, e). However, in hydrodynamically active environments, sediment particles are homogenous, and the sample from 15 cm depth had much finer particles and closer arrangement (Fig. 12b) compared to lower depths. These results suggest that the hydrodynamic contribution to sediment strength during consolidation can be attributed to particle composition changes and structure of the seabed sediments.

For seabed sediments with more cohesive particles, excess pore pressure may build up progressively and become equal to the effective overburden weight during cyclic loading, resulting in liquefaction or fluidisation of sediments (Wit and Kranenburg 1997; van Kessel and Kranenburg 1998). A hydraulic seepage gradient due to differences in excess pore pressure at different depths will cause the vertical migration of fine particles and corresponding changes in particle composition and structure of seabed sediments (Simon and

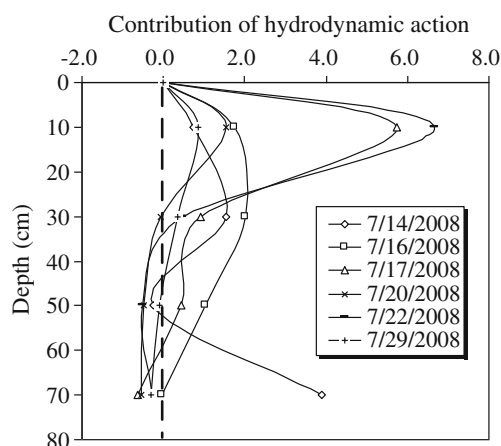
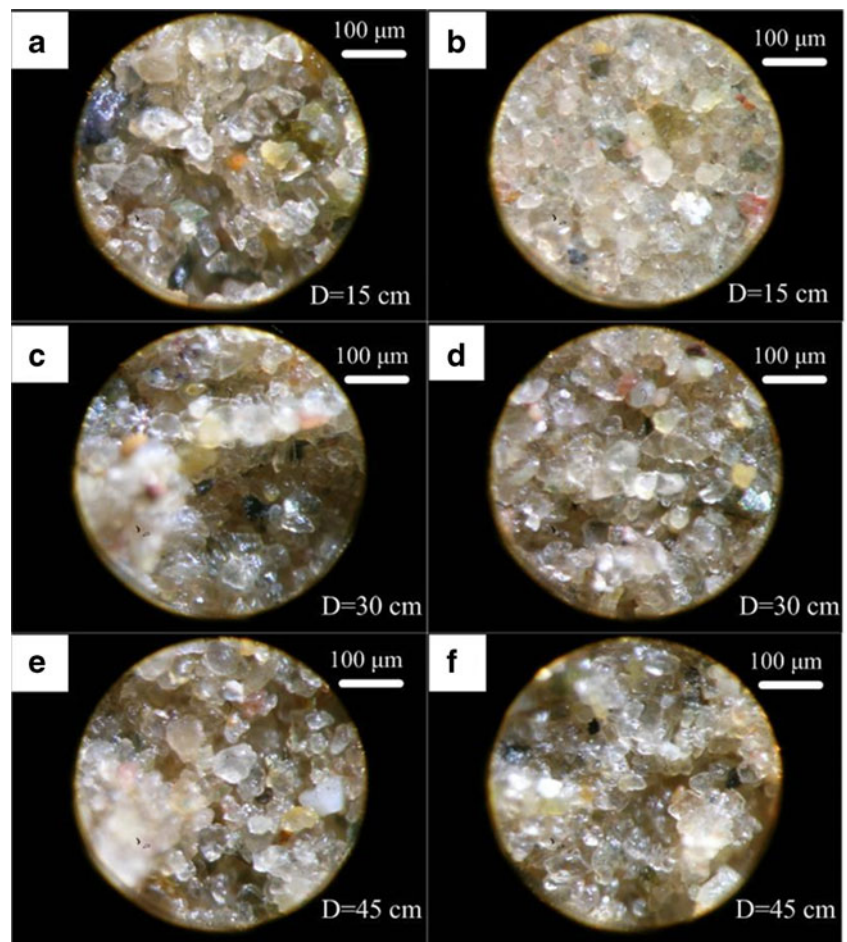


Fig. 11 Depth distribution curves of contribution of hydrodynamic action to sediment strength in the process of consolidation. The contribution values are the ratios calculated by subtracting the undrained shear strength in the covered plot from undrained shear strength in the open plot, and then dividing the result by undrained shear strength in the covered plot

Fig. 12 Microstructure images ($\times 180$) of sediments at different depths below the seabed surface: **a, c, e** collected from the covered plot; **b, d, f** collected from the open plot



Collison 2001). Variations in the strength of freshly deposited sediments are expected when hydrodynamics are seasonal or climate-driven, which may explain the long-term consolidation behaviour of sediments deposited from 2004 through 2008. The results suggest vertical migration of fine particles due to wave-induced seabed changes (Fig. 12) but are not conclusive because small-scale spatial variability in sediment condition and unquantified benthic bioturbation occur in the Yellow River delta. However, previous studies and visual observations from a laboratory flume under controlled conditions support the hypothesis that sediment was sorted by vertical seepage and stabilised in the wave-induced fluidised layer (Xu et al. 2009; Liu et al. unpublished data). The uneven spatial distribution of sediment strength in the Yellow River delta (Jia et al. 2011) is also related to wave-induced secondary modification of seabed sediments. This factor must be considered in morphodynamic models for intertidal mudflat sediments.

5.3 Sediment properties control erodibility

Results from this study offer some insight into the implications of consolidation of deposited sediments on controlling erosion in nearshore mudflats. Erosion is often dependent on

the magnitude and frequency of hydrodynamic forces, which generate sufficient shear stress to initiate seabed sediment erosion and transport superficial fine particles (e.g. Tanaka et al. 1995; Hemer et al. 2004). However, variations in sediment erosion resistance (i.e. erodibility) for some seabeds, during interactions between waves and sediments, have been demonstrated in some studies (e.g. Watts et al. 2003; Aberle et al. 2004; Stevens et al. 2007) but is generally less studied. Based on the wave-sediment interactions described by Jeng (2003), waves can change sediment erodibility by transforming sediment properties, such as undrained shear strength and penetration resistance (Fig. 10). Critical shear stress is an important parameter for describing the erosion resistance of seabed sediment. It is a complex function of shear strength, clay content, structure and other geotechnical properties (Parchure and Mehta 1985; Amos and Mosher 1985). However, the influence of wave-induced seabed changes on bottom sediment properties must be considered in sediment erosion and suspension models (Lambrechts et al. 2010). Variations in the threshold velocity, critical shear stress, undrained shear strength, and penetration strength with the cycle number of wave loading in field experiments (Fig. 10) also suggest a significant correlation between sediment erodibility and strength.

Therefore, further investigation of the relationship between sediment erodibility (i.e. threshold velocity and critical shear stress) and strength parameters (i.e. undrained shear strength and penetration resistance) for the Yellow River (Fig. 13) is needed. Plotting sediment undrained shear strength and penetration resistance against threshold velocity (Figs. 13a, b) shows a positive correlation:

$$u = 5.410 \ln(c_u) + 1.955 \text{ (cm/s)} \quad (R^2 = 0.94) \quad (3)$$

$$u = 3.971 \ln(p_s) + 9.459 \text{ (cm/s)} \quad (R^2 = 0.83) \quad (4)$$

where u is the threshold velocity, above which erosion is initiated; c_u is the undrained shear strength (kPa), and P_s is the penetration resistance (N) determined in field experiments. As expected, critical shear stress (τ_0) and sediment strength (Figs. 13c, d) are positively correlated:

$$\tau_0 = 0.039 \ln(c_u) - 0.019 \text{ (N/m}^2\text{)} \quad (R^2 = 0.96) \quad (5)$$

$$\tau_0 = 0.029 \ln(p_s) + 0.035 \text{ (N/m}^2\text{)} \quad (R^2 = 0.83) \quad (6)$$

This result is consistent with the correlation between critical shear stress and sediment shear strength (Watts et al. 2003). Thus, sediment erodibility can be characterised by easily-acquired sediment strength parameters for any consolidation conditions, despite complex wave-induced changes.

Wang et al. (2006) presents a wave-climate model for the modern Yellow River delta and concludes that some areas will experience increasing erosion with increasing storm intensity due to significant shear stress. However, wave-induced fluidisation and concurrent sediment densification complicate the response of sediment erosion resistance to hydrodynamic actions. Hence, further advances in results

interpretations, together with additional information on hydrodynamic and climatic behaviours, are needed to develop a proper erosion model. These models can play a key role in describing sediment dynamics in the Yellow River delta region.

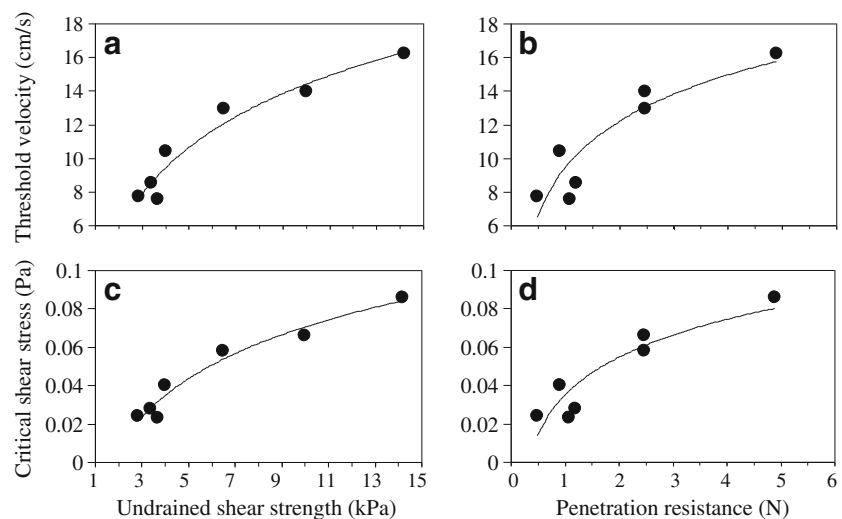
6 Conclusions

This paper presents new information on the consolidation of sediments discharged from the Yellow River. A continuous, 5-year survey of an intertidal mudflat in the Yellow River delta included excess pore pressure, sediment strength, and hydrodynamics measurements, as well as laboratory experiments on different temporal–spatial scales. The goal of this research was to describe short- and long-term consolidation behaviour and investigate the impacts of hydrodynamics on the erodibility of marine deposited sediments. These factors must be considered in morphodynamic models for intertidal mudflat sediments.

Results of this study suggest that sediments discharged from the Yellow River experience a high rate of consolidation after deposition. Excess pore water pressure dissipates completely after approximately 45 to 51 h, and the deposited sediments are then in a state of normal consolidation. Sediment strength continues to increase, and deposited sediments are thixotropic due to the evolution of particle structures.

Hydrodynamic action is crucial to sediment consolidation in the primary period and plays a decisive role in the development of stiff strata. The effect of hydrodynamic conditions on sediment strength is nearly seven times larger than that of self-weighting of the deposited sediments. The contribution of hydrodynamics to sediment strength during consolidation can be attributed to changes in particle composition and the structure of seabed sediments. Wave-induced seabed structure may

Fig. 13 Relationship between sediment erodibility and strength parameters: **a** threshold velocity vs. undrained shear strength, **b** threshold velocity vs. penetration resistance, **c** critical shear stress vs. undrained shear strength, and **d** critical shear stress vs. penetration resistance. Data marked (filled circle) indicates results measured in the erodibility experiments



explain the long-term consolidation behaviour of deposited sediments from 2004 to 2008.

Results from this study also offer some insights into erosion processes in nearshore mudflats and the implications of consolidation of deposited sediments. Under simulated wave conditions, there was a positive correlation between sediment erodibility (i.e. threshold velocity and critical shear stress) and strength parameters (i.e. undrained shear strength and penetration resistance). Sediment consolidation under hydrodynamic forcing directly determines the erosion resistance of seabed sediments. However, the impact of hydrodynamics on long-term patterns of sediment dynamics remains unclear due to several complicating factors, especially small-scale spatial variability in sediment condition and unquantified benthic bioturbation. Further advances in results interpretations, along with additional information regarding hydrodynamic and climatic behaviour, are needed to develop a proper erosion model of the Yellow River delta and other coastal environments.

Acknowledgments This study was jointly funded by the National Natural Science Foundation of China (Contract No. 40876042 and No. 41072215) and the National High Technology Research and Development Program of China (863 Program; Contract No. 2008AA09Z109). The authors would like to thank Professor J. Paul Liu for his revision on the English in this paper. The authors also appreciate the constructive comments from the editors and anonymous reviewers, which greatly improved the science and quality of our original manuscript.

Reference

- Aberle J, Nikora V, Walters R (2004) Effects of bed material properties on cohesive sediment erosion. *Mar Geol* 20(7):83–93
- Allen JRL (1997) Simulation models of salt marsh morphodynamics: some implications for high intertidal sediment couplets related to sea-level changes. *Sediment Geol* 113(3–4):211–223
- Amos CL, Mosher DC (1985) Erosion and deposition of fine-grained sediments from the Bay of Fundy. *Sedimentol* 32:815–832
- Amos CL, Daborn GR, Christian H, Atkinson A, Robertson A (1992) In situ measurements on fine-grained sediments from the Bay of Fundy. *Mar Geol* 108:175–196
- Anthony EJ (2004) Sediment dynamics and morphological stability of estuarine mangrove swamps in Sherbro Bay, West Africa. *Mar Geol* 208(2–4):207–224
- Berlamont J, Ockenden M, Toorman E, Winterwerp J (1993) The characterisation of cohesive sediment properties. *Coast Eng* 21(1–3):105–128
- Black K, Cramp A (1995) A device to examine the in situ response of intertidal cohesive sediment deposits to fluid shear. *Cont Shelf Res* 15(15):1945–1954
- Bornhold BD, Yang ZS, Keller GH, Prior DB, Wiseman WJ, Wang Q, Wright LD, Xu WD, Zhuang ZY (1986) Sedimentary framework of the modern Huanghe (Yellow River) delta. *Geo-Mar Lett* 6(2):77–83
- Busch WH, Keller GH (1982) Consolidation characteristics of sediments from the Peru-Chile continental margin and implications for past sediment instability. *Mar Geol* 45(1–2):17–39
- Capo S, Sottolichio A, Brenon I, Castaing P, Ferry L (2006) Morphology, hydrography and sediment dynamics in a mangrove estuary: The Konkoure Estuary, Guinea. *Mar Geol* 230(3–4):199–215
- Chang FQ (2009) Study on Mechanism of wave-induced Submarine Landslide at the Yellow River Estuary, China. Dissertation, Ocean University of China
- Coleman JM, Walker HJ, Grabau WE (1978) Sediment Instability in the Mississippi River Delta. *J Coast Res* 14(3):872–881
- Costanza R, D'Arge R, DeGroot R, Farber S, Grasso M, Hannon B, Limburg K, Naeem S, O'Neill RV, Paruelo J, Raskin RG, Sutton P (1997) The value of the world's ecosystem services and natural capital. *Nat* 387:253–260
- Davidson-Arnott RGD, Langham DRJ (2000) The effects of softening on nearshore erosion of cohesive shoreline. *Mar Geol* 166(1–4):145–162
- Deloffre J, Lafite R, Lesueur P, Lesourd S, Verney R, Guézennec L (2005) Sedimentary processes on an intertidal mudflat in the upper macrotidal Seine estuary, France. *Estuar Coast Shelf Sci* 64(4):710–720
- Dias CRR, Alves AML (2009) Geotechnical properties of the Cassino Beach mud. *Cont Shelf Res* 29(3):589–596
- Eisma D (1998) Intertidal Deposits: River Mouth, Tidal Flats, and Coastal Lagoons. CRC Press, Boca Raton, p 459
- Ender R (2009) Sediment physical properties of the DYNAS study area. *J Mar Syst* 75(3–4):317–329
- Fan H, Huang H, Zeng TQ, Wang K (2006) River mouth bar formation, riverbed aggradation and channel migration in the modern Huanghe (Yellow) River delta, China. *Geomorphol* 74(1–4):124–136
- Gong XN, Xiong CX, Xiang KX, Hou YF (2000) The formation of clay structure and its influence on mechanical characteristic of clay. *J Hydraulic Eng* (10): 43–47 (in Chinese, with English abstract)
- Gouleau D, Jouanneau JM, Weber O, Sauriau PG (2000) Short- and long-term sedimentation on Montportail Brouage intertidal mudflat, Marennes-Oléron Bay (France). *Cont Shelf Res* 20(12–13):1513–1530
- Hemer MA, Harris PT, Coleman R, Hunter J (2004) Sediment mobility due to currents and waves in the Torres Strait-Gulf of Papua region. *Cont Shelf Res* 24:2297–2316
- Janssen-Stelder B (2000) The effect of different hydrodynamic conditions on the morphodynamics of a tidal mudflat in the Dutch Wadden Sea. *Cont Shelf Res* 20(12–13):1461–1478
- Jeng DS (2003) Wave-induced sea floor dynamics. *Appl Mech Rev* 56(4):407–429
- Jia YG, Liu XL, Shan HX, Zheng JW, Huo SX (2011) The effects of hydrodynamic conditions on geotechnical strength of the sediment in Yellow River Delta, China. *Int J Sediment Res* 26(3):318–330
- Jia YG, Shan HX, Yang XJ, Meng XM, Chang FQ, Zheng JW (2012) Sediment dynamics and geologic hazards in the estuary of Yellow River. Science Press, Beijing, China
- Keller GH, Prior DB (1986) Sediment dynamics of the Huanghe (Yellow River) delta and neighboring gulf of Bohai, People's Republic of China: project overview. *Geo-Mar Lett* 6(2):63–66
- Keller GH, Zhen J, Yang ZS, Bornhold BD, Prior DB, Suhayda JN Jr, Wiseman WJ, Wright LD (1990) Mass physical properties of Huanghe delta and Southern Bohai Sea near-surface deposits, China. *Mar Georesour Geotechnol* 9(3):207–225
- Lambrechts J, Humphrey C, Mckinna L, Gourage O, Fabricius KE, Mehta AJ, Lewins S, Wolanski E (2010) Importance of wave-induced bed liquefaction in the fine sediment budget of Cleveland Bay, Great Barrier Reef. *Estuar Coast Shelf Sci* 89:154–162
- Liu XL, Jia YG, Zheng JW, Hou W, Zhang L, Zhang LP, Shan HX (2013) Experimental evidence of wave-induced inhomogeneity in

- the strength of silty seabed sediments: Yellow River Delta, China. *Ocean Eng* 59:120–128. doi:10.1016/j.oceaneng.2012.12.003
- Lu NZ, Suhayda JN, Prior DB, Bornhold BD, Keller GH Jr, Wiseman WJ, Wright LD, Yang ZS (1991) Sediment thixotropy and submarine mass movement, Huanghe delta, China. *Geo-Mar Lett* 11(1):9–15
- Meng XM, Jia YG, Hou W, Liu H, Yang ZN (2010) Study on erodibility change of the Yellow River sediment into the sea in the process of consolidation. Proceedings of the ASME 29th International Conference on Ocean, Offshore and Arctic Engineering, Shanghai, China 1:757–765
- Milliman JD, Meade RH (1983) World-wide delivery of river sediment to the ocean. *J Geol* 91:1–22
- Milliman JD, Syvitski JPM (1992) Geomorphic/tectonic control of sediment discharge into the ocean: the importance of small mountainous rivers. *J Geol* 100:525–544
- Morgan JP, Coleman JM, Gagliano SM (1963) Mudlumps at the mouth of South Pass, Mississippi River: sedimentology, paleontology, structure, origin, and relation to deltaic processes. Louisiana State University Press, Baton Rouge 10:190–215
- Neumeier U, Lucas CH, Collins M (2006) Erodibility and erosion patterns of mudflat sediments investigated using an annular flume. *Aquat Ecol* 40:543–554
- Parchure TM, Mehta AJ (1985) Erosion of soft cohesive sediment deposits. *J Hydraul Eng* 111:1308–1326
- Qiao S, Shi X, Zhu A, Liu Y, Bi N, Fang X, Yang G (2010) Distribution and transport of suspended sediments off the Yellow River (Huanghe) mouth and the nearby Bohai Sea. *Estuar Coast Shelf Sci* 86:337–344
- Quaresma VS, Bastos AC, Amos CL (2007) Sedimentary processes over an intertidal flat: A field investigation at Hythe flats, Southampton Water (UK). *Mar Geol* 241(1–4):117–136
- Ren M, Shi Y (1986) Sediment discharge of the Yellow River (China) and its effect on the sedimentation of the Bohai and the Yellow Sea. *Cont Shelf Res* 6(6):785–810
- Richardson MD, Briggs KB, Bentley SJ, Walter DJ, Orsi TH (2002) The effects of biological and hydrodynamic processes on physical and acoustic properties of sediments off the Eel River, California. *Mar Geol* 182(1–2):121–139
- Saito Y, Yang Z, Hori K (2001) The Huanghe (Yellow River) and Changjiang (Yangtze River) deltas: a review on their characteristics, evolution and sediment discharge during the Holocene. *Geomorphol* 41(2–3):219–231
- Shan HX, Liu H, Jia YG, Meng XM (2009) Effects of bioturbation on the erodibility of intertidal sediments in the Yellow River estuary, China. *Far East J Ocean Res* 2(3):157–170
- Shi MC, Zhao JP, Sun YY (1985) The analyses of hydrographical characteristic in estuary of Huanghe River. *Period Ocean Univ China* 15(2):81–95, in Chinese, with English abstract
- Shi C, Zhang D, You L, Li B, Zhang Z, Zhang O (2007) Land subsidence as a result of sediment consolidation in the Yellow River delta. *J Coast Res* 23(1):173–181
- Simon A, Collison AJC (2001) Pore-water pressure effects on the detachment of cohesive streambeds: seepage forces and matrix suction. *Earth Surf Process Landforms* 26:1421–1442
- Stevens AW, Wheatcroft RA, Wiberg PL (2007) Seabed properties and sediment erodibility along the western Adriatic margin, Italy. *Cont Shelf Res* 27:400–416
- Talke SA, Stacey MT (2003) The influence of oceanic swell on flows over an estuarine intertidal mudflat in San Francisco Bay. *Estuar Coast Shelf Sci* 58(3):541–554
- Tanaka H, van To D (1995) Initial motion of sediment under waves and wave-current combined motions. *Coast Eng* 25:153–163
- van Kessel T, Kranenburg C (1998) Wave-induced liquefaction and flow of subaqueous mud layers. *Coast Eng* 34(1–2):109–127
- van Maren DS, Winterwerp JC, Wang ZY, Pu Q (2009) Suspended sediment dynamics and morphodynamics in the Yellow River, China. *Sedimentol* 56(3):785–806
- Wang YH (2003) The intertidal erosion rate of cohesive sediment: a case study from Long Island Sound. *Estuar Coast Shelf Sci* 56(5–6):891–896
- Wang ZY, Liang ZY (2000) Dynamic characteristics of the Yellow River mouth. *Earth Surf Process Landf* 25(7):765–782
- Wang H, Yang Z, Li G, Jiang W (2006) Wave climate modeling on the abandoned Huanghe (Yellow River) delta lobe and related deltaic erosion. *J Coast Res* 22(4):906–918
- Wang H, Yang Z, Saito Y, Liu JP, Sun X, Wang Y (2007a) Stepwise decreases of the Huanghe (Yellow River) sediment load (1950–2005): Impacts of climate change and human activities. *Glob Planet Ch* 57:331–354
- Wang HJ, Yang ZS, Li YH, Guo ZG, Sun XX, Wang Y (2007b) Dispersal pattern of suspended sediment in the shear frontal zone off the Huanghe (Yellow River) mouth. *Cont Shelf Res* 27:854–871
- Watts CW, Tolhurst TJ, Black KS, Whitmore AP (2003) In situ measurements of erosion shear stress and geotechnical shear strength of the intertidal sediments of the experimental managed realignment scheme at Tollesbury, Essex, UK. *Estuar Coast Shelf Sci* 58:611–620
- Wheatcroft RA, Borgeld JC (2000) Oceanic flood deposits on the northern California shelf: large-scale distribution and small-scale physical properties. *Cont Shelf Res* 20(16):2163–2190
- Wit PJ, Kranenburg C (1997) The wave-induced liquefaction of cohesive sediment beds. *Estuar Coast Shelf Sci* 45(2):261–271
- Xu G, Sun Y, Wang X, Hu G, Song Y (2009) Wave-induced shallow slides and their features on the subaqueous Yellow River delta. *Can Geotech J* 46(12):1406–1417
- Yang Z, Ji Y, Bi N, Lei K, Wang H (2011a) Sediment transport off the Huanghe (Yellow River) delta and in the adjacent Bohai Sea in winter and seasonal comparison. *Estuar Coast Shelf Sci* 93:173–181
- Yang Z, Shan H, Jia Y, Meng X, Zheng J (2011b) Erosion-deposition evolution characteristics of north beach in Yellow River Delta. *Chin J Geotech Eng* 33:152–162
- Zheng J, Shan H, Jia Y, Liu X, Hou W (2011) Field tests and observation of wave-loading influence on erodibility of silty sediments in the Huanghe (Yellow River) estuary, China. *J Coast Res* 27(4):706–717